



Article

# Study on the Properties of Cement-Based Cementitious Materials Modified by Nano-CaCO<sub>3</sub>

Chonggen Pan <sup>1,\*</sup> , Jiawei Zang <sup>2</sup>, Keyu Chen <sup>1</sup>  and Jingge Ren <sup>1</sup>

<sup>1</sup> Department of Civil Engineering, School of Civil Engineering & Architecture, NingboTech University, No. 1 Qianhu South Road, Yinzhou, Ningbo 315100, China

<sup>2</sup> Department of Structural Engineering, College of Civil Engineering and Architecture, Zhejiang University, No. 866 Yuhangtang Road, Xihu, Hangzhou 311400, China

\* Correspondence: panchonggen@zju.edu.cn

**Abstract:** The effects of Nano-CaCO<sub>3</sub> on the physical, mechanical properties and durability of cement-based materials were investigated in this paper. The mechanical property, durability and SEM microscopic tests of test blocks with different Nano-CaCO<sub>3</sub> content were carried out. Results showed that Nano-CaCO<sub>3</sub> could improve the flexural strength, compressive strength and impermeability of cement-based materials. When the content of Nano-CaCO<sub>3</sub> is 2.0%, the strengthening effect of Nano-CaCO<sub>3</sub> on the cement-based materials was optimized, and the flexural strength of cement-based materials after 3 d, 7 d and 28 d increased by 12.6%, 18% and 32.4%, respectively, compared with the reference group. When the content of Nano-CaCO<sub>3</sub> exceeded 2.0%, the flexural strength of cement-based materials begins to decline with the increase of Nano-CaCO<sub>3</sub> content. Similarly, when the content of Nano-CaCO<sub>3</sub> reached 2.0%, the impermeability of the cement-based materials was also optimized, and the permeability height of the base group could be increases by 41.4%. At the early stage of hydration, the exothermic rate of cement with 2.0% Nano-CaCO<sub>3</sub> content was higher than that of other contents. When the content of Nano-CaCO<sub>3</sub> increased from 0 to 2.0%, the hydration exothermic rate increased gradually with the increase of Nano-CaCO<sub>3</sub> content.

**Keywords:** durability; microstructure; hydration; multiscale; bending toughness



**Citation:** Pan, C.; Zang, J.; Chen, K.; Ren, J. Study on the Properties of Cement-Based Cementitious Materials Modified by Nano-CaCO<sub>3</sub>. *Appl. Sci.* **2023**, *13*, 2451. <https://doi.org/10.3390/app13042451>

Academic Editor: Chao-Wei Tang

Received: 7 December 2022

Revised: 9 January 2023

Accepted: 13 January 2023

Published: 14 February 2023



**Copyright:** © 2023 by the authors. Licensee MDPI, Basel, Switzerland. This article is an open access article distributed under the terms and conditions of the Creative Commons Attribution (CC BY) license (<https://creativecommons.org/licenses/by/4.0/>).

## 1. Introduction

Cement-based materials, which are the most prevalent building materials, have excellent performance in economy, molding, energy saving and durability, etc. However, traditional cement-based materials have the disadvantages of excessive dead load, easy to crack and low tensile strength, limiting their application to a certain extent [1]. High performance cement-based materials (HPC) with high compressive strength and durability overcome some of the disadvantages of ordinary cement-based materials. However, some deficiencies are present in the toughness, tension and compression (bending) ratio [2], crack resistance and so on. As a consequence, concrete structures often fail before the end of their design service life due to different environmental factors, and due to its low durability, has caused many casualties and economic losses [3].

The main factors that influence the durability of concrete structures in service include internal factors, external factors, and the hydration property of cementitious materials. The internal factors mainly include the poor structural uniformity of concrete, easily leading to uneven stress distribution, and low compactness resulting in insufficient impermeability, corrosion resistance and frost resistance [4–7]. The dominant external factors include physical effects (e.g., freeze-thaw cycle, dry-wet alternation and temperature change), and chemical effects (e.g., environmental medium corrosion, carbonization, alkali–aggregate reactions, reinforcement corrosion) [4]. In addition, the composition and stability of the hydration products of cementitious materials are important factors affecting its durability, such that the instability and decomposition of the gel that makes up the structure gradually

loosens until it collapses. Therefore, improving the properties of hydration products of cementitious materials is a more controllable and manageable method to increase the durability of concrete structures.

In the early 1990s, Taylor, a British scholar, found that 70% of cement hydration products were calcium-silicate-hydrate (C-S-H) gel, and the cement slurry was composed of primarily nanomaterials condensed by C-S-H gel particles on a microscopic level [8]. Xiaozhong Zhang [9] and G Richardson [10] et al. found that the specific surface area of C-H-S gel was about  $180 \text{ m}^2 \cdot \text{g}^{-1}$ , and the average particle size of C-S-H gel was about 10 nm, which sets up a theoretical basis for the study of cement-based materials on the nanometer scale. Through the nano-modification of cement-based materials, we could further optimize the microstructure of cement-based materials, so as to strengthen the mechanical properties and durability of concrete structures.

The main mechanism of nanomaterials on the acceleration of hydration is to react with  $\text{Ca}(\text{OH})_2$  and speed up the formation of C-S-H gel. The majority of studies [11–14] have focused on nanosilica. The addition of Nano- $\text{SiO}_2$  could effectively decrease the content of free  $\text{Ca}(\text{OH})_2$  in cement paste [15] and cement mortar [16], through reacting with  $\text{Ca}(\text{OH})_2$  and reducing the ion exchange between the matrix and the external environment. As a result, the leakage of  $\text{Ca}^{2+}$  can be controlled and the stability of the microstructure can be improved. Except for nanosilica, other nanomaterials have been investigated, including Nano- $\text{CaCO}_3$  [17], nanoclays [18], titanium dioxide [19], carbon nanotubes [20], graphene nanoplates [21,22] etc. T. Sato et al. [23] found that Nano- $\text{CaCO}_3$  could significantly accelerate the early hydration reaction, in which the accelerating effect is positively proportional to the dosage. The promotion was mainly found to be attributed to the acceleration of the hydration of  $\text{C}_3\text{S}$  and the formation of the dominant hydration product, C-S-H gel, through the reaction of Nano- $\text{CaCO}_3$  and  $\text{Ca}(\text{OH})_2$ , by the same group people and their colleagues [24].

Except for speeding up the hydration, other modifications have been studied by adding various nanomaterials, such as to the compressive strength [24–27], deformation capacity and durability [24–26], corrosion resistance [28] and electrical conductivity and wave-absorbing properties [29]. With the addition of 1% and 3% Nano- $\text{SiO}_2$ , the compressive strength of cement-based materials at 28 days could be increased by about 50%, and the deformation capacity and durability of cement-based materials were also significantly improved [24–26]. Li Guhua et al. [30] studied the performance changes of Nano- $\text{SiO}_2$ -modified concrete under the condition of a salt crystallization cycle by SEM (scanning electron microscope) and XRD (X-ray diffraction). They found that the corrosion resistance cycle coefficient and relative corrosion resistance cycle coefficient of the modified concrete mixed with 1% Nano- $\text{SiO}_2$  were increased by 11% and 20%, respectively, after 110 cycles, compared with ordinary coagulation [30]. This indicates that Nano- $\text{SiO}_2$  could significantly improve the salt corrosion resistance of concrete. Xiong Guoxuan et al. [31] studied the effects of different mass fractions of Nano- $\text{TiO}_2$  on the electrical conductivity and wave-absorbing properties of the cement matrix, which showed that 5% Nano- $\text{TiO}_2$  had the most significant effect on the electrical conductivity and wave-absorbing properties of the cement matrix. Huang Zhengyu et al. [27] added Nano- $\text{CaCO}_3$  into ultra-high performance concrete, and studied its influence on the performance of ultra-high performance concrete, finding that Nano- $\text{CaCO}_3$  could improve the compressive strength and flexural strength of ultra-high performance concrete, reduce its fluidity and promote the hydration reaction.

At present, domestic and foreign scholars focus less on Nano- $\text{CaCO}_3$ -modified cement-based materials and, particularly, the combination of multi-scale fibers with nanomaterials, and more on single-fiber-modified cement-based materials. Therefore, based on the existing science and technology of concrete materials, low-priced Nano- $\text{CaCO}_3$  was adapted to carry out a nano-modification on the most critical components of cement-based materials. It is possible to prolong the service life of concrete members by refining the grain, regulating the microstructure, improving the strength and the anti-deterioration performance of the structure matrix of cement-based materials. The synergistic effect among nanomaterials

and cementitious materials brings the mortar advantages of high strength, high toughness and high crack resistance. At the same time, this research can play a significant role in concrete structures used in architectural engineering for protecting against corrosive media, improving durability, and also have important practical engineering significance for ensuring the service safety of structures.

## 2. Raw Materials and Specimens Preparation

### 2.1. Raw Materials

#### (1) Cement

P·O 42.5 ordinary Portland cement produced by Zhejiang Qianchao Holding Co., Ltd., Hangzhou, China was used. Its specific surface area is about 315 m<sup>2</sup>/kg and has a specific gravity of 3.14. The particle size distribution, microstructure and mineral phase composition of cement are shown in Figures 1–3. It can be observed that the cement particles are distributed unevenly in small pieces or flakes, of which the main mineral phase groups are quartz, calcite, Portland stone and so on.

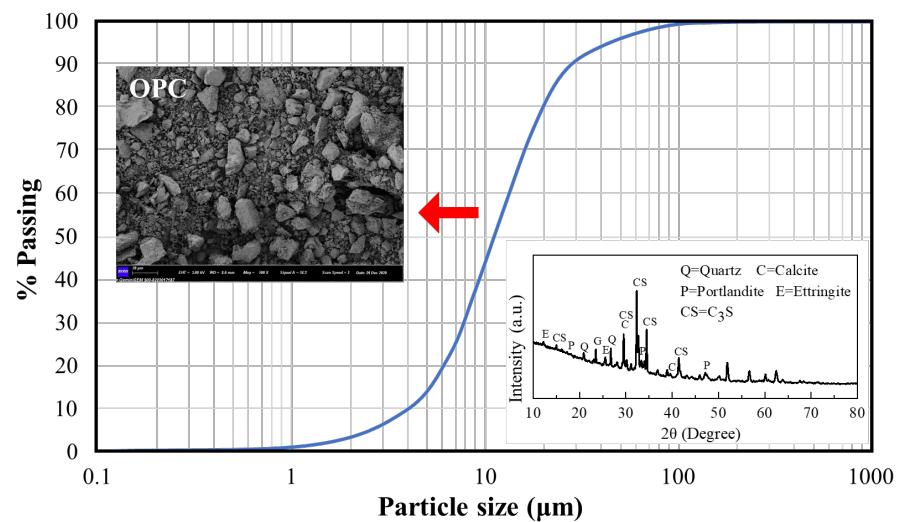


Figure 1. Portland cement grading curve.

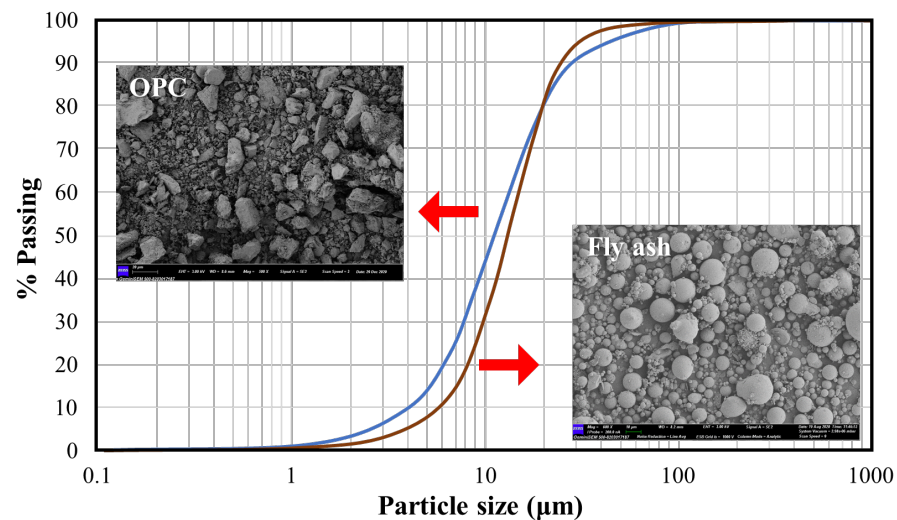


Figure 2. Portland cement grading curve.

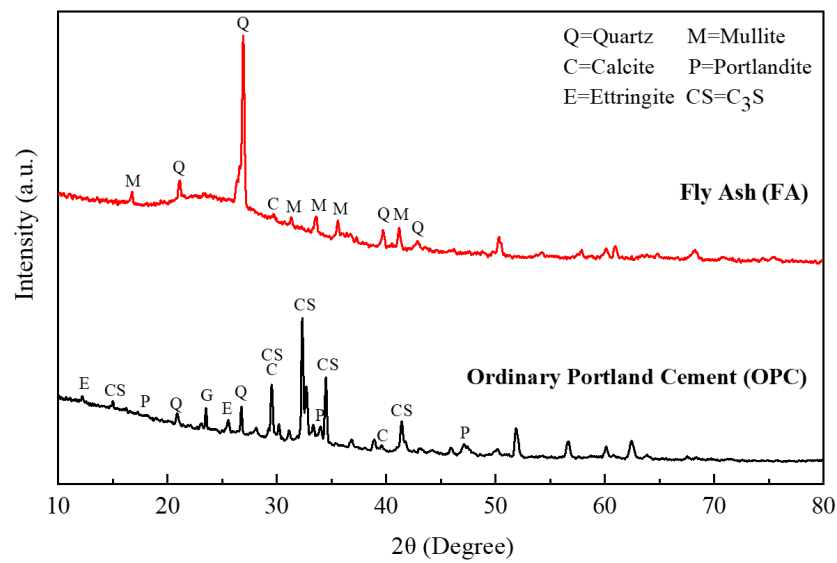


Figure 3. Mineral phase of Portland cement.

(2) Sand

ISO sand (GB/T17671) with a specific gravity of 2.67 and a fineness modulus of 2.68 was used.

(3) Nano-CaCO<sub>3</sub>

The Nano-CaCO<sub>3</sub> used in this paper was proceeded by Shanghai Yuanjiang Chemical Co., Ltd., Shanghai, China Its fineness modulus is a 5000 mesh (Figure 4), and the specific indicators are shown in Table 1.

Table 1. Indicators of Nano-CaCO<sub>3</sub>

Inspection Items	Physical Index (\%)	Inspection Results (\%)	Conclusion
Content of CaCO <sub>3</sub>	98	98.5	qualified
Whiteness	95 ± 2	95	qualified
Fineness (5000) sieve residue	≤0.05	0.030	qualified
Content of water	≤0.5	0.15	qualified
PH of water suspension	6.5~7.5	7.5	qualified
Oil absorption value	26 ± 5	28	qualified



Figure 4. Nano-CaCO<sub>3</sub>.

#### (4) Water reducing agent

A high-performance polycarboxylic acid water reducer with a water reduction rate of 25% was used.

#### (5) Fly ash

Fly ash with a fineness of 43  $\mu\text{m}$ , a density of 2.4  $\text{g}/\text{cm}^3$  and a water content of 0.5% was used.

### 2.2. Specimens Preparation

#### 2.2.1. Design of Mixture Ratio

P-O 42.5 ordinary Portland cement was selected in this test. The mix proportions used in the test is shown in Table 2.

**Table 2.** Test mix ratios of cement-based materials with different contents of Nano- $\text{CaCO}_3$ .

Number	Water Cement Ratio	Cement (g)	Fly Ash (g)	Sand (g)	Content of Nano $\text{CaCO}_3$ (%)	Water Reducing Agent (g)	Water (g)
0	0.3	300	100	200	0.0	10	120
1	0.3	300	100	200	0.5	10	120
2	0.3	300	100	200	1.0	10	120
3	0.3	300	100	200	2.0	10	120
4	0.3	300	100	200	3.0	10	120
5	0.3	300	100	200	4.0	10	120

#### 2.2.2. Preparation and Curing of Test Pieces

Nano- $\text{CaCO}_3$  is easy to agglomerate because of its high specific surface area and surface energy, hindering the promotion of Nano- $\text{CaCO}_3$  during the cement hydration process [32]. Therefore, the dispersion degree of Nano- $\text{CaCO}_3$  is particularly important in the application process. We weighed and added the fly ash, sand, cement and Nano- $\text{CaCO}_3$  into the mixer in sequence and stirred for 3 min to disperse the Nano- $\text{CaCO}_3$  evenly. Then we added the water reducing agent and water, and continued to stir for 3 min. After mixing, we poured the slurry into the mold, and placed it into a standard curing box with a temperature of  $20 \pm 5$   $^\circ\text{C}$  and a relative humidity of 65%. The formwork was removed 24 h later, and curing continued to the corresponding age (e.g., 3 d, 7 d, and 28 d).

### 3. Characterization Test

#### 3.1. Mechanical Property Test

The compressive and flexural strengths of the specimens at three curing ages (i.e., 3 d, 7 d and 28 d) were tested according to the standard for test method of basic properties of construction mortar (JGJ/T70—2009) [27]. In the compressive strength test, the size of the compressive strength test specimens were  $70.7 \times 70.7 \times 70.7$  mm, and the pressure testing machine was a sye-300 (Zhejiang Zhongke Instrument Co., Ltd.) with an accuracy class of 1 and a maximum load of 10 kN. In the bending strength test, the size of the compressive strength test specimens were  $100 \times 100 \times 400$  mm, and the microcomputer controlled electronic bending and compression testing machine TYE-6 (Wuxi Jianyi Machinery Co., Ltd., Wuxi, China) had an accuracy class of 1 and maximum load of 10 kN. Three repeated test pieces were formed for compressive strength and flexural strength testing.

In the compression test, we applied a continuous load at a speed of 0.6–0.8 MPa/s. When the specimens began to deform rapidly and approached failure, we stopped adjusting the accelerator of the testing machine at the point of failure, and then recorded the failure load. The compressive strength of the test piece was calculated according to the follow-

ing formula (the measured compressive strength value is multiplied by the dimension conversion factor of 0.95):

$$f_c = \frac{F}{A} \quad (1)$$

where  $f_c$  represents the compressive strength (MPa),  $F$  represents the failure load (N) and  $A$  refers to the pressure bearing area ( $\text{mm}^2$ ), which was taken as  $4998.59 \text{ mm}^2$ .

In the bending test, we applied a continuous load at a speed of  $0.05\text{--}0.08 \text{ MPa/s}$ . When the specimens began to deform rapidly and approached failure, we stopped adjusting the accelerator of the testing machine at the point of failure, and then recorded the failure load. The bending strength of the test piece was calculated according to the following formula (the measured compressive strength value is multiplied by the dimension conversion factor of 0.85):

$$f_f = \frac{Fl}{bh^2} \quad (2)$$

where  $f_f$  (MPa) represents the bending strength,  $F$  (N) represents the failure load,  $l$  (mm) represents the span between supports (taken as  $300 \text{ mm}$  in this test),  $h$  (mm) represents the section height (taken as  $100 \text{ mm}$  in this test) and  $b$  (mm) represents the section width (taken as  $100 \text{ mm}$  in this test).

### 3.2. Impermeability Test

The metal test mold was a truncated conical metal test mold with a bottom, which has an upper opening diameter of  $70 \text{ mm}$ , a lower opening diameter of  $80 \text{ mm}$  and a height of  $30 \text{ mm}$ . After forming, the test specimens were de-moulded after standing at room temperature ( $20 \pm 5 \text{ }^\circ\text{C}$ ) for  $24 \pm 2 \text{ h}$ , and continued to cure to their corresponding curing ages in the curing room with a temperature of  $20 \pm 2 \text{ }^\circ\text{C}$  and a humidity of more than  $90\%$ . After curing and being dried, the specimens were sealed into the mortar penetrometer. Then, we performed the permeability test.

The water pressure remained at  $0.2 \text{ MPa}$  for  $2 \text{ h}$ , and was then increased by  $0.1 \text{ MPa/h}$ . When half of end faces of the specimens were permeable, we stopped the testing and the water pressure was recorded.

The mortar seepage pressure value was calculated by the maximum pressure when 4 out of the 6 test specimens in each group were no longer permeable, which was calculated according to the following formula:

$$P = H - 0.1 \quad (3)$$

where  $P$  represents the impermeability pressure of mortar and  $H$  represents the water pressure when 3 of the 6 test specimens were permeable.

### 3.3. Hydration Heat Test of Cement

$410 \text{ g}$  of nitric acid solution ( $13.5 \pm 0.5 \text{ }^\circ\text{C}$ ,  $2.00 \pm 0.02 \text{ mol/L}$ ) and  $80 \text{ mL}$  of  $40\%$  hydrofluoric acid were mixed before adding them into the thermos. Then  $7 \pm 0.001 \text{ g}$  of zinc oxide were added and readings from the thermometer over different periods were read for the calculation of heat capacity using a Bain thermometer. Four specimens of dehydrated cement ( $3 \pm 0.001 \text{ g}$ ) were prepared, 2 of which were added into the above acid and readings from the thermometer over different periods were read, while the others were burned in a furnace at  $900\text{--}950 \text{ }^\circ\text{C}$  for  $90 \text{ min}$  and subsequently weighed. The dissolution heat of the dehydrated cement was calculated.

The test specimens were cured for  $3 \text{ d}$ ,  $7 \text{ d}$ ,  $14 \text{ d}$  and  $28 \text{ d}$  and sieved under a  $0.60 \text{ mm}$  mesh after grounding. Four specimens of dehydrated cement ( $3 \pm 0.001 \text{ g}$ ) were prepared, and the heat of dissolution of the hydrated samples was calculated by the method described previously. Finally, the value for the heat of hydration was calculated.

### 3.4. SEM Microanalysis

In this experiment, the S-3500 scanning electron microscope (made in Japan) was used to observe the microstructure of cement samples. The reference group and two groups of test blocks with a Nano-CaCO<sub>3</sub> content of 2.0% were split to make the specimens such that each specimen had a diameter less than 2.2 mm and a height less than 1.6 mm for scanning electron microscope observation. The specimens were sprayed with gold to enable good conductivity. The specimens were bonded to the specimen seat with conductive adhesive, and the gold-plated sections of the specimens with natural fractures were taken as the observation surface.

## 4. Results and Discussion

### 4.1. Effect of Nano-CaCO<sub>3</sub> on the Mechanical Properties of Mortar

#### 4.1.1. Effect of Nano-CaCO<sub>3</sub> on the Compressive Strength of Mortar

Figure 5 demonstrates how the compressive strength of mortar varies with increasing amounts of added Nano-CaCO<sub>3</sub>. Similar in the case of flexural strength, when the content of Nano-CaCO<sub>3</sub> increases from 0 to 2.0%, the compressive strength of cement-based materials shows an increased positive correlation with the amount of Nano-CaCO<sub>3</sub>, peaking at 2.0% Nano-CaCO<sub>3</sub>. After 3 d, 7 d and 28 d of curing, compressive strength increased by 8.5%, 11.4 and 19.1%, respectively, compared with the reference group. When the content exceeded 2.0%, the compressive strength began to decrease.

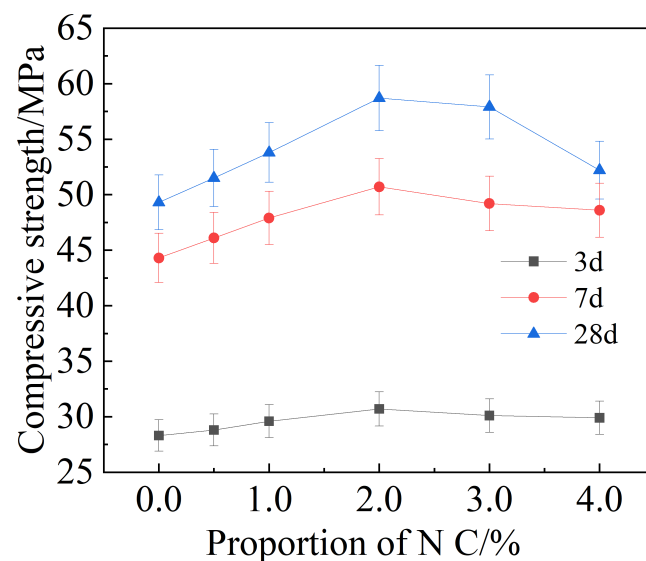
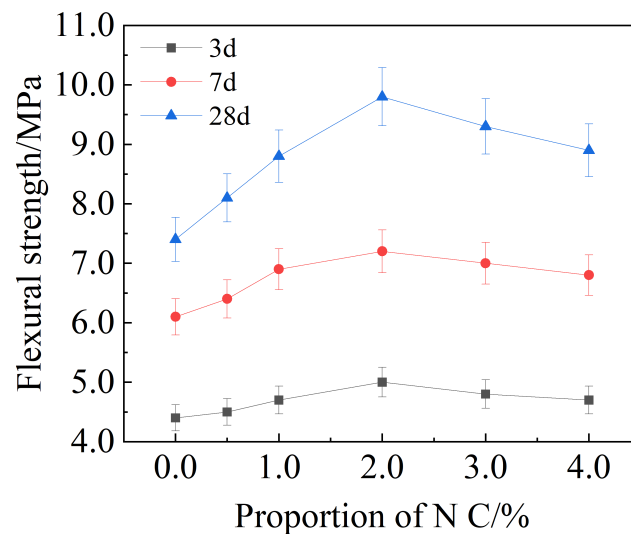


Figure 5. Compressive strength of mortar with different amounts of Nano-CaCO<sub>3</sub>.

It can be inferred that 2.0% is the optimal content of Nano-CaCO<sub>3</sub> in cement-based materials for the improvement of flexural and compressive strength.

#### 4.1.2. Effect of Nano-CaCO<sub>3</sub> on the Flexural Strength of Mortar

The flexural strength of mortar changes with increasing dosages of Nano-CaCO<sub>3</sub>, as is shown in Figure 6. When the content of Nano-CaCO<sub>3</sub> was increased to 2.0%, the flexural strength of cement-based materials after 3 d, 7 d and 28 d increased positively by 12.6%, 18 and 32.4%, respectively, compared with the reference group, and reached the maximum at 2.0% Nano-CaCO<sub>3</sub>. When the content exceeded 2.0%, the flexural strength began to decrease.



**Figure 6.** Flexural strength of mortar with different amounts of Nano-CaCO<sub>3</sub>.

#### 4.2. Effect of Nano-CaCO<sub>3</sub> on the Impermeability of Cement-Based Materials

After the penetration test was completed, we used the pressure testing machine to break the specimen, test the penetration height and calculate the average value. The average water seepage height of the test is shown in Figure 7.

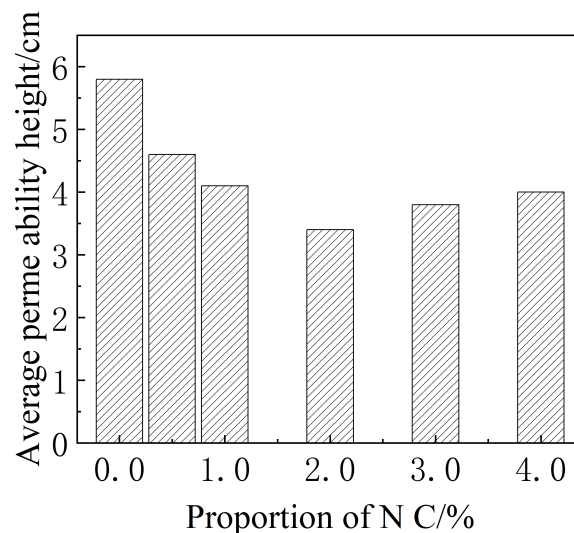


**Figure 7.** Average permeability height of mortar with different amounts of Nano-CaCO<sub>3</sub>.

There were weak permeability areas in the reference group and the water seepage height was uneven. The addition of Nano-CaCO<sub>3</sub> prolonged the penetration path of cement-based materials, making the water seepage height more uniform. It can be seen from Figure 7 that when the content of Nano-CaCO<sub>3</sub> was 2.0%, the penetration height could be increased by 41.4% compared with the reference group.

#### 4.3. Effect of Nano-CaCO<sub>3</sub> on the Hydration Heat of Cement

The influence of various amounts of Nano-CaCO<sub>3</sub> on the heat of hydration is presented in Figure 8. In the early stage of the hydration, the exothermic rate of cement with a Nano-CaCO<sub>3</sub> content of 2.0% was the highest, and in the process of the Nano-CaCO<sub>3</sub> content increasing from 0 to 2.0%, the rate of the hydration exothermic heat increased gradually with the increase of Nano-CaCO<sub>3</sub> content. An explanation can be that the high specific



surface area of Nano-CaCO<sub>3</sub> caused a nucleation effect, promoting cement hydration and releasing a lot of heat.

In the later stage of hydration, C-S-H gel and Ca(OH)<sub>2</sub> were coated around the clinker particles, which hindered the reaction of water and clinker particles and delayed the hydration. At the same time, the hydration heat in specimens after 3 d with 0%, 0.5%, 1.0%, 2.0%, 3.0% and 4.0% Nano-CaCO<sub>3</sub> accounted for 27.9%, 30.7%, 32.9%, 42.4%, 42.1% and 31.8% of the total hydration heat after 28 d, respectively. It was further proven that nanoparticles could accelerate the early hydration of cement, and the heat release rate is positively correlated with the content. In the figure, the heat release rate of Nano-CaCO<sub>3</sub> decreases significantly in the later stage, which was conducive to the release of the hydration heat of the cement.

Hydration heat at 28 d fluctuates at ~450 J/g with various contents of Nano-CaCO<sub>3</sub>, indicating that the addition of Nano-CaCO<sub>3</sub> does not affect the total amount of exothermic heat. Therefore, it could be inferred that nanoparticles were not directly involved in the hydration reaction. We therefore could infer that Nano-CaCO<sub>3</sub> would affect the mechanical properties of cement in the early stage of hydration.

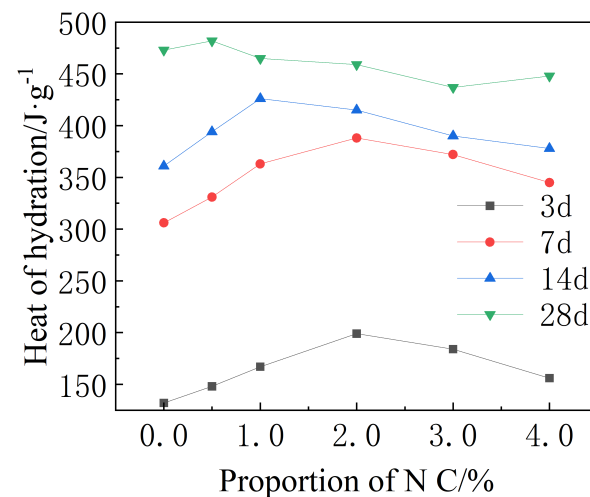


**Figure 8.** Hydration heat of cement-based materials with different amounts of Nano-CaCO<sub>3</sub> at different curing ages.

#### 4.4. SEM Microscopic and Mechanism Analysis

The hydration morphology of the samples with 0 and 2.0% Nano-CaCO<sub>3</sub> at the curing age of 28 d is shown in Figure 9.

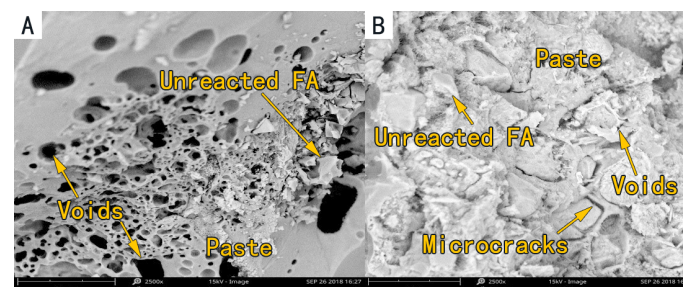


**Figure 9.** SEM image of a cement stone hydrated with 2.0% Nano-CaCO<sub>3</sub> (A) at 28 d and a blank sample (B).

It can be seen from Figure 9 that the cement paste of the base group with 0% Nano-CaCO<sub>3</sub> content had several large pores, whereas the sample with 2.0% Nano-CaCO<sub>3</sub> had a lesser amount of internal pores. The cement paste with 2.0% Nano-CaCO<sub>3</sub> content was more compact, in which a large number of high-strength cementitious substances were

formed. It can also be seen from Figure 10 that the content of ettringite (AFt) in the sample with 2% Nano-CaCO<sub>3</sub>, which could inhibit the hydration reaction, was less than that in the blank sample. The hydration reaction was more complete and the hydrated cementitious material was more predominant than in the blank sample, hence, the structural density was better and the mechanical properties were stronger.

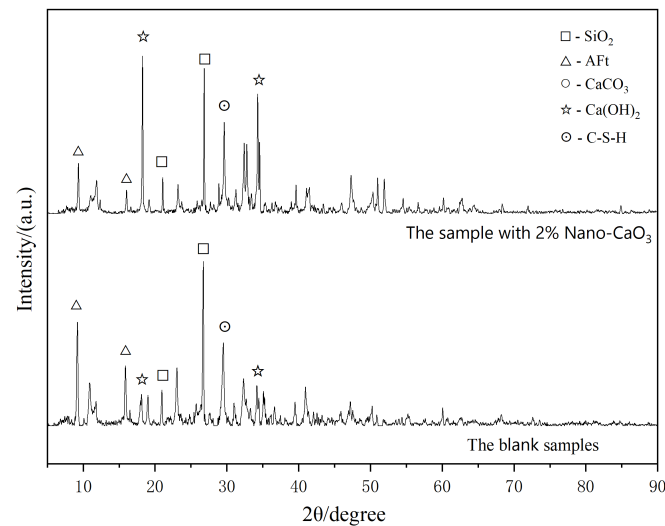


**Figure 10.** XRD pattern of Cement stone hydrated with 2.0% Nano-CaCO<sub>3</sub> (A) for 28 d and the blank sample (B).

The main way for Nano-CaCO<sub>3</sub> to affect the strength of cement-based materials is to improve the strength of cement paste [29] through the small-size effect and the surface effect [33]. Combined with the SEM test results, we could infer that Nano-CaCO<sub>3</sub> could accelerate the hydration of cement, optimize the interface structure of cement stone, and improve the compactness [34]. Finally, the strength of cement paste was improved.

The promotion mechanism of Nano-CaCO<sub>3</sub> on hydration reaction in concrete is shown in Figure 11. The high specific surface area and surface energy of Nano-CaCO<sub>3</sub> brought high surface activity. In the initial stage of hydration, C<sub>3</sub>S was hydrated and released a large amount of Ca<sup>2+</sup>. The surfaces of Nano-CaCO<sub>3</sub> would physically adsorb Ca<sup>2+</sup> [35], promoting the nucleation of nearby Nano-Ca(OH)<sub>2</sub> and grow in large quantities on the surface of Nano-CaCO<sub>3</sub> particles, so as to accelerate the hydration of C<sub>3</sub>S, which was particularly significant in the early stage of hydration [16]. At the same time, Nano-CaCO<sub>3</sub> could further bind to the cement hydration product, C-H-S, and form ettringite (AFt) with a microcrystalline nucleus of itself. Monosulfide hydrated calcium sulphoaluminate (AFm) and the C-S-H gel phase strengthened the structure and shape of the micro interface layer, and effectively enhanced the mechanical properties of the hardened cement paste [36–39].

In the later stage of hydration, a large amount of Nano-CaCO<sub>3</sub> coating around the clinker particles would react with the aluminum phase (C<sub>3</sub>A) in the cement to form the hydration product single carbon hydrated calcium carboaluminate (3CaOAl<sub>2</sub>O<sub>3</sub>CaCO<sub>3</sub>12H<sub>2</sub>O), which hinders the hydration reaction by reducing the direct contact with clinker and water. The more the content percentage, the more obvious the hindering effect was. Therefore, Nano-CaCO<sub>3</sub> could not promote the later hydration of cement-based materials [40], and the strength of cement-based materials would decrease with the increase of Nano-CaCO<sub>3</sub> content. In addition, too much Nano-CaCO<sub>3</sub> would hinder the transformation of AFt to AFm, and the expanded internal stress produced by a large amount of AFt would destroy the structure of hardened cement slurry and reduce the strength of the cement-based materials.

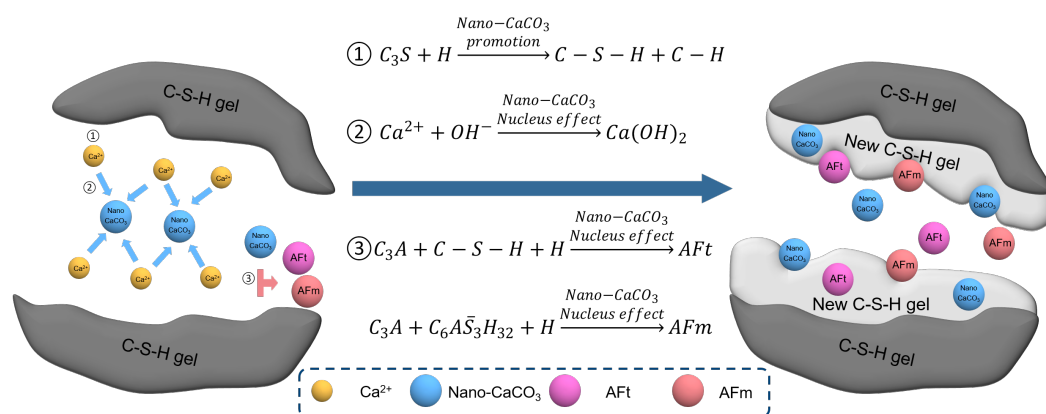


**Figure 11.** Mechanism of Nano- $\text{CaCO}_3$  improving cementitious materials.

## 5. Conclusions

In this paper, the effect of Nano- $\text{CaCO}_3$  on the physical and mechanical properties of cement-based cementitious materials was studied through micro and macro tests, and the reinforcement mechanisms of Nano- $\text{CaCO}_3$  on cement-based cementitious materials were analyzed. The main conclusions are as follows:

(1) The proper addition of Nano- $\text{CaCO}_3$  could improve the strength of cement-based materials. When the content of Nano- $\text{CaCO}_3$  was 2%, the flexural strength, compressive strength and impermeability reached their respective peaks;

(2) Nano- $\text{CaCO}_3$  could accelerate the hydration of early cement. According to the SEM microscopic test, it could be seen that Nano- $\text{CaCO}_3$  could fill the pores of cement-based materials, inhibiting the growth of needle shaped ettringite and promoting the formation of high-strength gel, which made the cement paste more compact and enhanced the strength of the cement paste.

(3) Using Nano- $\text{CaCO}_3$  to modify cement-based cementitious materials could significantly improve the durability of cement-based cementitious materials, indicating that nanomaterials have broad prospects in construction engineering [41]. In addition, this field needs further research and expansion. In particular, the effects of Nano- $\text{CaCO}_3$  on cement hydration and the change of interface properties of cement-based materials are not clear and require further study.

**Author Contributions:** C.P.: statement of Conceptualization, Methodology; J.Z.: Data curation, Writing- Original draft preparation; K.C.: Writing- Reviewing and Editing; J.R.: Writing- Reviewing and Editing. All authors have read and agreed to the published version of the manuscript

**Funding:** The authors gratefully acknowledge the Natural Science Foundation of Zhejiang Province (Grant No. LGG21E080006), Science and technology project of the Ministry of housing and urban rural development (2021-k-117), Ningbo 2025 Science and Technology Major Project (Grant No. 2019B10049, 2020Z035, 2020Z040).

**Institutional Review Board Statement:** We declare that the research content of this paper does not involve ethical issues.

**Informed Consent Statement:** In this paper, the authors declared that they have no conflicts of interest to this work. We declare that we do not have any commercial or associative interest that represents conflict of interest in connection with the work submitted.

**Data Availability Statement:** Some or all data, models, or code that support the findings of this study are available from the corresponding author upon reasonable request. All data, models, and code generated or used during the study appear in the submitted article.

**Conflicts of Interest:** In this paper, the authors declared that they have no conflicts of interest related to this work, nor any commercial or associative interests that represent potential conflicts of interest in connection with the work submitted.

## References

1. Zhao, G.; Peng, S.; Huang, C. *Steel Fiber Reinforced Concrete Structure*; China Architecture & Building Press: Beijing, China, 1999; pp. 45–48.
2. Zhao, G. *Advanced Reinforced Concrete Structure*; China Electric Power Press: Beijing, China, 1999.
3. Jin, Z.; Gu, J.; Hou, B. Inspection and Assessment of Concrete Structure Durability of Coastal Bridge. *J. Highw. Transp. Res. Dev.* **2010**, *27*, 58–62.
4. Moreno, M.; Morris, W.; Alvarez, M.G.; Duffó, G.S. Corrosion of reinforcing steel in simulated concrete pore solutions effect of carbonation and chloride content. *Corros. Sci.* **2004**, *46*, 2681–2699. [[CrossRef](#)]
5. Liu, Z.; Hansen, W. Pore damage in cementitious binders caused by deicer salt frost exposure. *Constr. Build. Mater.* **2015**, *98*, 204–216. [[CrossRef](#)]
6. Li, F.; Yuan, Y.; Li, C.Q. Corrosion propagation of prestressing steel strands in concrete subject to chloride attack. *Constr. Build. Mater.* **2011**, *25*, 3878–3885. [[CrossRef](#)]
7. Zhang, T.; Yu, Q.; Wei, J.; Zhang, P. Efficient utilization of cementitious materials to produce sustainable blended cement. *Cem. Concr. Compos.* **2012**, *34*, 692–699. [[CrossRef](#)]
8. Taylor, H.F.W. *Cement Chemistry*; Thomas Telford: London, UK, 1997.
9. Zhang, X.; Chang, W.; Zhang, T.; Ong, C. Nanostructure of calcium silicate hydrate gels in cement paste. *J. Am. Ceram. Soc.* **2000**, *83*, 2600–2604. [[CrossRef](#)]
10. Richardson, I. Nature of C-S-H in hardened cements. *Cem. Concr. Res.* **1999**, *29*, 1131–1147. [[CrossRef](#)]
11. Shih, J.Y.; Chang, T.P.; Hsiao, T.C. Effect of nanosilica on characterization of Portland cement composite. *Mater. Sci. Eng. A* **2006**, *424*, 266–274. [[CrossRef](#)]
12. Jo, B.W.; Kim, C.H.; Tae, G.h.; Park, J.B. Characteristics of cement mortar with Nano-SiO<sub>2</sub> particles. *Constr. Build. Mater* **2007**, *21*, 1351–1355. [[CrossRef](#)]
13. Nazari, A.; Riahi, S. The effects of SiO<sub>2</sub> nanoparticles on physical and mechanical properties of high strength compacting concrete. *Compos. Part B Eng.* **2011**, *42*, 570–578. [[CrossRef](#)]
14. Qing, Y.; Zenan, Z.; Deyu, K.; Rongshen, C. Influence of Nano-SiO<sub>2</sub> addition on properties of hardened cement paste as compared with silica fume. *Constr. Build. Mater* **2007**, *21*, 539–545. [[CrossRef](#)]
15. Gaitero, J.; Campillo, I.; Guerrero, A. Reduction of the calcium leaching rate of cement paste by addition of silica nanoparticles. *Cem. Concr. Res.* **2008**, *38*, 1112–1118. [[CrossRef](#)]
16. Arefi, M.R.; Javaheri, M.R.; Mollaahmadi, E.; Zare, H.; Eskandari, M. Silica nanoparticle size effect on mechanical properties and microstructure of cement mortar. *J. Am. Sci.* **2011**, *7*, 231–238.
17. Sato, T.; Beaudoin, J. Effect of Nano-CaCO<sub>3</sub> on hydration of cement containing. *Adv. Cem. Res.* **2010**, *23*, 1–29.
18. Chang, T.P.; Shih, J.Y.; Yang, K.M.; Hsiao, T.C. Material properties of Portland cement paste with nano-montmorillonite. *J. Mater. Sci.* **2007**, *42*, 7478–7487. [[CrossRef](#)]
19. Jayapalan, A.R.; Lee, B.Y.; Fredrich, S.M.; Kurtis, K.E. Influence of Additions of Anatase TiO<sub>2</sub> Nanoparticles on Early-Age Properties of Cement-Based Materials. *Transp. Res. Rec. J. Transp. Res. Board* **2010**, *2141*, 41–46. [[CrossRef](#)]
20. Adhikary, S.; Rudzionis, Ž.; Tučkutė, S.; Ashish, D.K. Effects of carbon nanotubes on expanded glass and silica aerogel based lightweight concrete. *Sci. Rep.* **2021**, *11*, 2104. [[CrossRef](#)] [[PubMed](#)]
21. Adhikary, S.K.; Rudzionis, Z.; Tuckute, S. Characterization of aerogel and EGA-based lightweight cementitious composites incorporating different thickness of graphene platelets. *J. Build. Eng.* **2022**, *57*, 104870. [[CrossRef](#)]
22. Adhikary, S.K.; Rudzionis, Z.; Ghosh, R. Influence of CNT, graphene nanoplate and CNT-graphene nanoplate hybrid on the properties of lightweight concrete. *Mater. Today Proc.* **2021**, *44*, 1979–1982. [[CrossRef](#)]
23. Sato, T.; Diallo, F. Seeding effect of Nano-CaCO<sub>3</sub> on the hydration of tricalcium silicate. *Transp. Res. Rec. J. Transp. Res. Board* **2010**, *2141*, 61–67. [[CrossRef](#)]
24. Ye, Q. Comparison of pozzolanic activity between nano-SiO<sub>2</sub> and powder and chemical coagulation. *Cem. Concr. Compos.* **2001**, *3*, 19–21.
25. Ye, Q.; Zhang, Z.; Chen, R.; Chengchang, M. Interaction of Nano-CaCO<sub>3</sub> with portlandite at interface between hardened cement paste and aggregate. *J. Chin. Ceram. Soc.* **2003**, *31*, 517–522.
26. Ye, Q.; Zhang, Z.; Kong, D.; Chen, R.; Ma, C. Comparison of performance of high-strength coagulation with Nano-SiO<sub>2</sub> and powder. *J. Build. Mater.* **2003**, *6*, 381–385.
27. Huang, Z.; Zu, T. Influence of Nano-CaCO<sub>3</sub> on Ultra High Performance Concrete. *Bull. Chin. Ceram. Soc.* **2013**, *32*, 1103–1125.
28. China Academy of Building Research. *JGJ/T70—2009; Standard for Test Method of Basic Properties of Construction Mortar*. China Architecture & Building Press: Beijing, China, 2003.
29. Yang, J. Study on the performance of Nano-CaCO<sub>3</sub> modified cement concrete. *New Build. Mater.* **2019**, *46*, 52–54.
30. Li, Y.; Gao, B. Effect of nano-SiO<sub>2</sub> on crystallization cycle performance of coagulation main salts. *J. Southwest Jiaotong Univ.* **2007**, *42*, 70–74.
31. Xiong, G.; Deng, M.; Xu, L.; Tang, M. Properties of Cement-Based Composites by Doping Nano-TiO<sub>2</sub>. *J. Chin. Ceram. Soc.* **2006**, *34*, 1158–1161.
32. Song, X.; Wang, H.; Wu, X.; Feng, Q. Research and Development of Dispersion Technique for Nanoparticles. *Chem. Ind. Eng. Prog.* **2005**, *1*, 47–52.

33. Wang, X.; Lu, L. Progress of preparation and applications of metal oxide nanocrystallines. *Chin. J. Inorg. Chem.* **2000**, *16*, 213–217.
34. Hu, H.; Yan, C.; He, Z.; Li, Z.; Zhan, P. Progress of Preparation and Applications of Metal Oxide Nanocrystallines. *China Concr. Cem. Prod.* **2020**, *6*, 94–97.
35. ROY, D. New strong cement materials: Chemically bonded ceramics. *Science* **1987**, *235*, 651–658. [[CrossRef](#)] [[PubMed](#)]
36. Diao, M.; Sun, X.; Wei, C.; Zhao, Y. Analysis of compressive strength and meso numerical simulation of Nano-CaCO<sub>3</sub> reinforced concrete. *J. Qinghai Univ.* **2021**, *39*, 69–76+112.
37. Qu, C.; Sun, Y.; Zhang, P. Effect of Nano-CaCO<sub>3</sub> on mechanical properties of recycled aggregate concrete. *Concrete* **2020**, 82–84+87.
38. Sun, Y. *Study on the Effect of Nano-CaCO<sub>3</sub> on Concrete Performance*; Qingdao University of Technology: Qingdao, China, 2018.
39. Wang, D. Effect of Nano-CaCO<sub>3</sub> on properties of cement. *Build. Mater. Technol. Appl.* **2017**, 1–3.
40. Wu, H.; Sun, L.; Chen, K.; Wei, J. Study on impermeability of cement mortar mixed with Nano-SiO<sub>2</sub>. *Highway* **2020**, *65*, 241–244.
41. Xiao, J.; Zhou, S.; Shen, C.; Li, Y. Research Progress on the Effect of Nano-CaCO<sub>3</sub> on the Properties of Cement Concrete. *Build. Technol.* **2018**, *2*, 80–84.

**Disclaimer/Publisher’s Note:** The statements, opinions and data contained in all publications are solely those of the individual author(s) and contributor(s) and not of MDPI and/or the editor(s). MDPI and/or the editor(s) disclaim responsibility for any injury to people or property resulting from any ideas, methods, instructions or products referred to in the content.